Ordering in the dilute weakly anisotropic antiferromagnet $Mn_{0.35}Zn_{0.65}F_2$

F. C. Montenegro
Departamento de Fisica, Universidade Federal de Pernambuco, 50670-901 Recife PE, Brazil

D. P. Belanger and Z. Slanič
Department of Physics, University of California, Santa Cruz, California 95064

J. A. Fernandez-Baca
Solid State Division, Oak Ridge National Laboratory, Oak Ridge, Tennessee 37831-6393

(Received 28 July 1999)

The highly diluted antiferromagnet $Mn_{0.35}Zn_{0.65}F_2$ has been investigated by neutron scattering in zero field. The Bragg peaks observed below the Néel temperature ($T_N \approx 10.9$ K) indicate stable antiferromagnetic (AF) long-range ordering at low temperature. The critical behavior is compatible with random-exchange Ising model critical exponents ($\nu \approx 0.69$ and $\gamma \approx 1.31$), as reported for $Mn_xZn_{1-x}F_2$ with higher x and for the isostructural compound $Fe_xZn_{1-x}F_2$. However, in addition to the Bragg peaks, unusual scattering behavior appears around the (1 0 0) AF Bragg peak below a glassy temperature $T_g \approx 7.0$ K. The glassy region $T < T_g$ corresponds to that of noticeable frequency dependence in earlier zero-field ac susceptibility measurements on this sample. These results indicate that long-range order coexists with short-range nonequilibrium clusters in this highly diluted magnet.

Diluted uniaxial antiferromagnets have been extensively studied as physical realizations of theoretical models of random magnetism,[1] including those pertaining to percolation phenomena.[2,3] For three dimensions ($d=3$), two of the most extensively studied examples are the rutile compounds $Mn_xZn_{1-x}F_2$ and $Fe_xZn_{1-x}F_2$. These two systems differ effectively only in the strength and nature of the anisotropy, providing a unique opportunity to explore the role of anisotropy in the ordering of dilute magnets at low temperature. In $Mn_xZn_{1-x}F_2$, the anisotropy is dipolar in origin.[4] In $Fe_xZn_{1-x}F_2$, the anisotropy is an order of magnitude greater for $x=1$ because of the additional crystal-field contribution.[5] In many experiments with the magnetic concentration x well above the percolation threshold concentration $x_p=0.245$,[2] the behaviors for $H=0$ are qualitatively similar for $Mn_xZn_{1-x}F_2$ and $Fe_xZn_{1-x}F_2$. Antiferromagnetic (AF) long-range order (LRO) at low temperatures and characteristic random-exchange Ising critical behavior have been observed in the $Fe_xZn_{1-x}F_2$ compounds for $x \geqslant 0.31$.[6] Similar random-exchange Ising-model (REIM) behavior is found in the $Mn_xZn_{1-x}F_2$ system for $x > 0.4$.[7]

For small fields applied parallel to the uniaxial direction and reasonably small magnetic dilution, the diluted antiferromagnet in a field (DAFF) is expected[8,9] to show critical behavior belonging to the same universality class as the random-field Ising model (RFIM) for the ferromagnet, the latter being the model most used in simulations.[10] Indeed, for all measured samples of both systems for which the REIM character is found at $H=0$, the application of a small field parallel to the easy axis generates critical behavior compatible with the predicted[8] REIM to RFIM crossover scaling. In spite of the evidence supporting the DAFF as a realization of the RFIM, some nonequilibrium features inherent to DAFF compounds and also the newly explored field limits[11–13] of the weak RFIM problem in $d=3$ make the nature of the phase transition at $T_c(H)$ still a matter of considerable controversy.[14–16]

Under strong random fields (corresponding to large H) and also close to the percolation threshold, the phase diagrams of DAFF's have proven to be much more complicated than originally anticipated. For large H, AF LRO is predicted to become unstable.[17] The generation of strong random fields induces[18,19] a glassy phase in the upper part of the (H,T) phase diagram of $d=3$ Ising DAFF's. The equilibrium boundary,

$$T_{eq}(H) = T_N - bH^2 - C_{eq}H^{2/\phi}, \tag{1}$$

above which hysteresis is not observed, has a convex shape at high $H(\phi > 2)$, instead of the concave ($\phi = 1.4$) curvature seen at low field (where REIM to RFIM crossover occurs). This change of curvature in T_{eq} vs H was first observed[20] by magnetization measurements in $Fe_{0.31}Zn_{0.69}F_2$. Faraday rotation[6] and neutron scattering[21] experiments on a sample with the same x confirmed the REIM to RFIM crossover scaling at low H and the lack of stability of the AF LRO at large H, giving way to a random-field-induced glassy phase in this highly diluted compound. Recent magnetization measurements indicated that similar structure in the phase diagram exists at very high fields for samples with higher values of x.[11,12] At a still higher concentration, the low-temperature hysteresis observed for $x < 0.8$ is absent.[22]

The magnetic features observed at large H in samples of $Fe_xZn_{1-x}F_2$ in the concentration range $0.3 < x < 0.6$ contrast with the behavior in the weakly anisotropic system $Mn_xZn_{1-x}F_2$ for intermediate x, where a strong H induces a spin-flop phase.[23] This distinct behavior may be solely a consequence of the stronger Ising character of the former system. In the strong dilution regime ($x \approx x_p$), a number of mag-

netic features lead us to distinguish between these two systems, as well. For $x \leqslant 0.27$, no long-range order[24] is observed in $Fe_xZn_{1-x}F_2$. Typical spin-glass behavior was found[25] in a sample with $x=0.25$, although recent works[26–28] suggest noncritical dynamics for x close to x_p in this system. Close to the percolation threshold, even a minute exchange frustration is a suitable mechanism[29] for the spin-glass phase in $Fe_xZn_{1-x}F_2$, as supported by local mean-field simulations.[30] For Ising systems, it is also expected that the dynamics even at zero field should be extremely slow.[31] In $Mn_xZn_{1-x}F_2$, ac susceptibility measurements indicate a spin-glass clustering at low temperatures for samples with Mn concentrations $0.2<x<0.35$.[32,36] Earlier neutron-scattering studies[37] suggest, however, that at $H=0$ the termination of the line of the AF-paramagnetic (P) continuous phase transition occurs at $T=0$ at $x=x_p$, in stark contrast to the behavior of $Fe_{0.25}Zn_{0.75}F_2$. In light of this contrast, the influence of the frozen spin-glass clusters on the stability of the AF LRO for x close to x_p in $Mn_xZn_{1-x}F_2$ is an important question that motivated the present work. The dipolar anisotropy of this weakly anisotropic system is expected to become random in strength and direction as x decreases, in contrast to the x-independent single-ion anisotropy of $Fe_xZn_{1-x}F_2$. In the case of $Mn_xZn_{1-x}F_2$ under strong dilution, the application of the results from numerical simulations[30] applied to Ising systems is, of course, not warranted. Any differences observed in this system and the $Fe_{0.31}Zn_{0.69}F_2$ must certainly reflect the difference in anisotropy, and this may give a window to the understanding of the general phase diagrams for dilute anisotropic antiferromagnets in applied fields.

In this study, we performed zero-field neutron-scattering experiments in $Mn_{0.35}Zn_{0.65}F_2$ to verify the existence of a stable long-range-ordered antiferromagnetic phase below a critical temperature $T_N \approx 10.9$ K, where REIM critical exponents $\nu \approx 0.69$ and $\gamma \approx 1.31$ are compatible with the behavior, and to investigate the dynamic features of the system at low temperature. Below $T_g \approx 7.0$ K, an unusual scattering behavior appears for $(1\ q\ 0)$ for $|q|>0$, where (1 0 0) is the antiferromagnetic Bragg peak. This temperature regime corresponds to the region where earlier ac susceptibility studies[36] indicated a noticeable frequency dependence in the real part of the susceptibility, in the absence of external field. The results indicate that long-range order coexists with nonequilibrium clusters in this highly diluted system.

The neutron-scattering experiments were performed at the Oak Ridge National Laboratory using the HB2 spectrometer in a two-axis configuration at the High Flux Isotope Reactor. We used the (002) reflection of pyrolytic graphite to monochromate the beam at 14.7 meV. This energy is sufficient to ensure that the static approximation is well satisfied for the range of correlation lengths probed.[33] The collimation was 60 min of arc before the monochromator, 40 min between the monochromator and sample, and 40 min after the sample. A pyrolitic graphite filter reduced higher-energy neutron contamination. The c axis of the crystal was vertical. A small mosaic was observed from the Bragg-peak scans at low temperature, with roughly a half-width of 0.2 degrees of arc or 0.0035 reciprocal lattice units (rlu). The mosaic was incorporated into the resolution correction by numerically convoluting the measured resolution functions, including the mosaic, with the line shapes used in the data fits.[38] Most of the

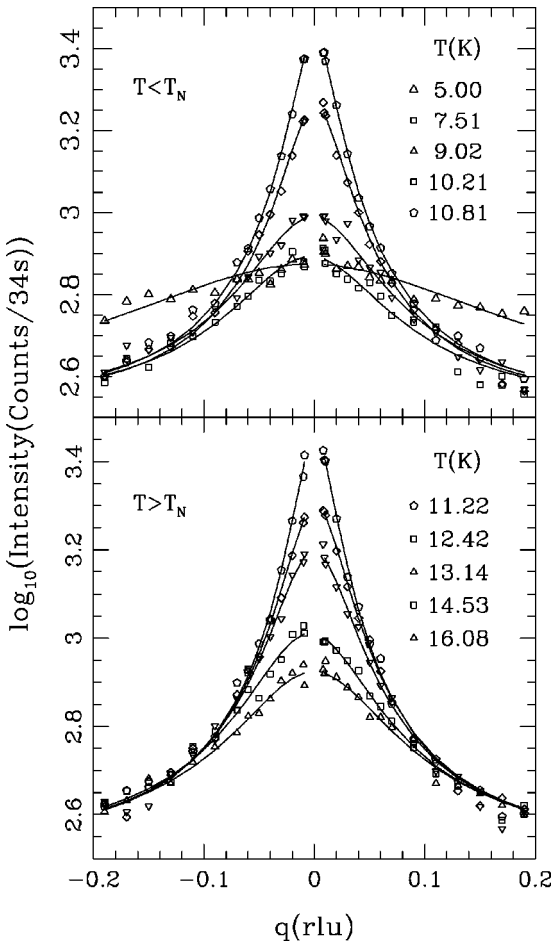

FIG. 1. The logarithm of the neutron-scattering intensity vs q just above and below T_N in zero field obtained after quenching the sample to $T=5$ K and heating.

scans taken were $(1\ q\ 0)$ transverse scans. For simplicity, the line shapes used in the fits to the data are of the mean-field form

$$S(q)=\frac{A}{q^2+\kappa^2}+M_s^2\delta(q), \tag{2}$$

where $\kappa=1/\xi$ is the inverse fluctuation correlation length and M_s is the Bragg scattering from the long-range staggered magnetization. The critical power-law behaviors are expected to be $\kappa=\kappa_0^{\pm}|t|^{\nu}$, $\chi=A\kappa^{-2}=\chi_0^{\pm}|t|^{-\gamma}$ and $M_s=M_0|t|^{\beta}$, where M_0 is nonzero only for $t<0$. The exponents ν, γ, and β and amplitude ratios κ_0^+/κ_0^- and χ_0^+/χ_0^- are universal parameters characterizing the random-exchange Ising model.

The sample was wrapped in aluminum foil and mounted on an aluminum cold finger. A calibrated carbon resistor was used to measure the temperature.

Transverse scans, taken after quenching to low temperatures ($T=5$ K) and subsequently heating the sample, are shown in Fig. 1. For clarity, the data for the range $|q|<0.008$ rlu, which spans the Bragg scattering component, are not shown. For the most part, the scans are quite consistent[35] with what is expected for a phase transition occurring near $T=11$ K. However, a most unusual feature of

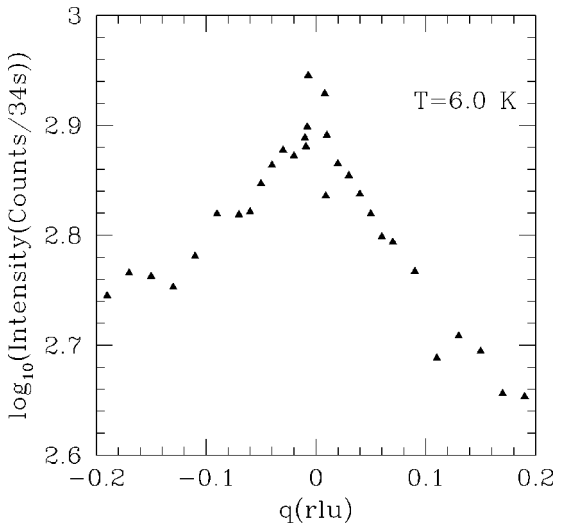

FIG. 2. The logarithm of the neutron-scattering intensity vs q for $T=6.00$ K in zero field obtained after quenching the sample to $T=5$ K and heating. The data were taken in sequence in increasing q with approximately 35 sec per point. The asymmetry indicates that on this time scale the system is relaxing toward the behavior seen at higher T.

the line shapes is evident in the data at the lowest temperature, $T=5$ K. The broad line shape indicates a great deal of short-range order present upon quenching. The short-range order is evident for the scans with $T<7$ K. The scan at $T=6$ K shows striking asymmetry, as shown in Fig. 2. Since the scans were taken with increasing q from -0.19 to 0.19 rlu and each measurement took about 35 sec, the asymmetry is an indication that the short-range order is rapidly decreasing with time, i.e., the system is equilibrating. The slow relaxation for $T<7$ K corresponds very well to the large frequency dependence observed using ac susceptibility in the same sample[36] for $T<7$ K.

A transition to antiferromagnetic long-range order is indicated by the presence of a resolution-limited Bragg scattering peak that decreases sharply as T approaches $T_N \approx 11$ K. As $T \rightarrow T_N$ from above, the width of the non-Bragg scattering component decreases and the $q=0$ intensity increases. Similarly, as $T \rightarrow T_N$ from below, the width decreases and the $q=0$ intensity increases. Such behavior is typical of an antiferromagnetic phase transition. To fit the data, we used the Lorentzian term in Eq. (1), convoluted with the instrumental resolution. The data for $|q|<0.008$ rlu were eliminated from the fits to the Lorentzian term to avoid Bragg scattering. The results of the fits yield $\kappa(T)$ and the staggered susceptibility $\chi(T)=A/\kappa^2$. The results for κ are shown in Fig. 3, along with the expected random-exchange critical behavior[39,40] as indicated by the solid curves with $\nu=0.69$ and $\kappa_0^+/\kappa_0^-=0.69$. The overall amplitude of the solid curves is adjusted to approximately follow the data. A clear minimum $\kappa \approx 0.017$ rlu is observed in the fitted values near T_N, indicating significant rounding due to a concentration gradient in the crystal.[41] The gradient rounding is most likely the cause of the deviations of the data from the fit away from the minimum as well. Nevertheless, the present data are plausibly consistent with random-exchange critical behavior when the significant rounding due to the concentration gradient is taken into account.

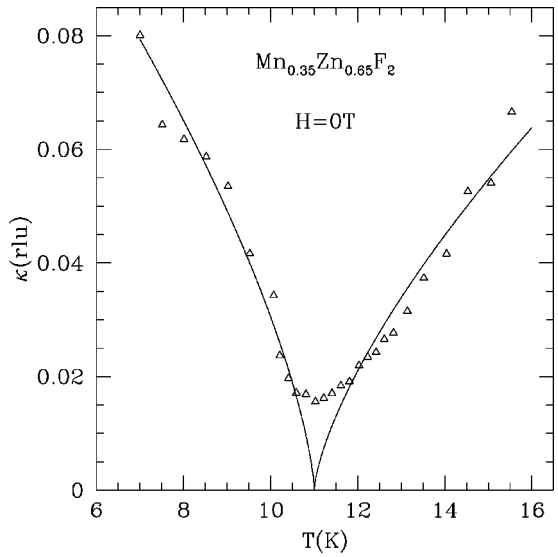

FIG. 3. κ vs T near T_N. The solid curves represent the expected random-exchange critical behavior.

Results for the logarithm of χ vs T are shown in Fig. 4. The random-exchange behavior,[39,40] with $\gamma=1.31$ and $\chi_0^+/\chi_0^-=2.8$ and with the overall amplitude adjusted to approximately fit the data, is shown as solid curves. The maximum in the data and the systematic deviations from the fit are indications of a significant gradient in the concentration, as we discussed with respect to Fig. 3. Again, the data are fairly consistent with a concentration-rounded random-exchange transition to antiferromagnetic long-range order.

The Bragg intensity, obtained by subtracting the fitted Lorentzian scattering intensity from the total $q=0$ scattering intensity, is shown vs T in Fig. 5. Once again, the data are fairly consistent with a random-exchange[42] transition ($\beta=0.35$) near $T=11$ K represented by the solid curve. The nonzero Bragg component above $T=11$ K is probably attributable mainly to concentration gradient effects. The precise shape of the Bragg scattering intensity vs T in Fig 5

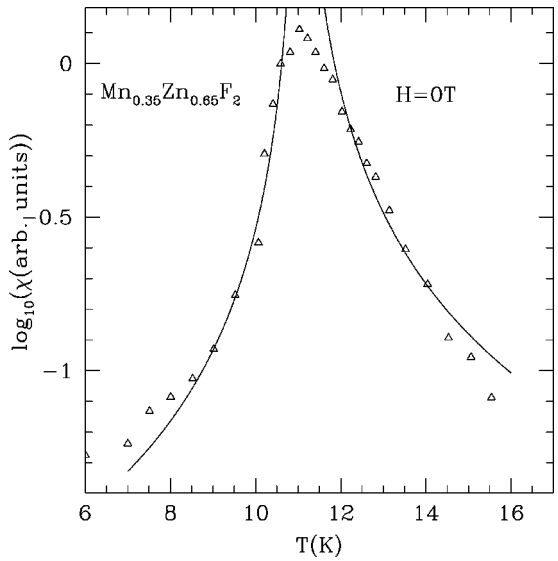

FIG. 4. The logarithm of χ vs T near T_N. The solid curves represent the expected random-exchange critical behavior.

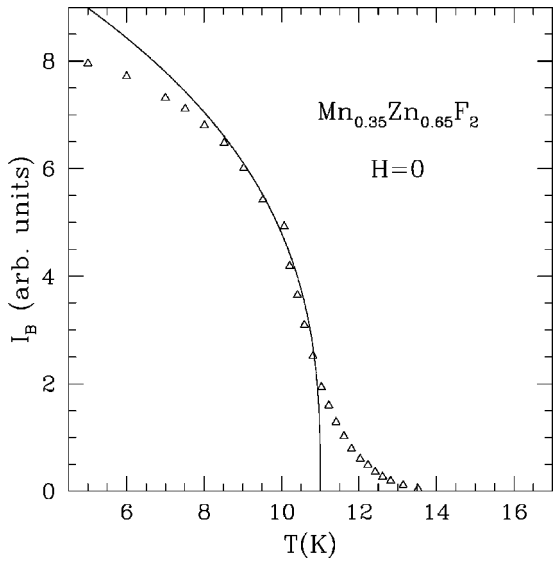

FIG. 5. The Bragg scattering intensity. The solid curves represent the expected random-exchange critical behavior vs T.

must not be taken too seriously, particularly at low T, since it is known that severe extinction effects distort the behavior by saturating the measured value.[1] In addition, for $T<7$ K, the sample shows nonequilibrium effects since it was quenched, as described above, and the magnitude of the Bragg scattering component might well be smaller than if the sample were in equilibrium. The large Bragg scattering component well below T_N, along with the minimum in κ and maximum in χ near T_N, strongly indicate an antiferromagnetically ordered phase.

Previous magnetization studies[23,36] indicate a de Almeida–Thouless-like curve in the H-T phase diagram. The $H=0$ end point of this boundary coincides reasonably well with the antiferromagnetic phase transition observed with neutron scattering.

In conclusion, we have shown neutron scattering evidence that this system, $Mn_{0.35}Zn_{0.65}F_2$, orders near $T=11$ K in a way consistent with the REIM model. In addition, significant relaxation takes place for $T<7$ K. This is consistent with previous magnetization measurements and demonstrates that only part of the system orders with long-range order when the system is quenched to low temperatures. This behavior is consistent with clusters coexisting with long-range order below T_N. A similar glassy low-temperature region has been identified[6,20,28] in the anisotropic system $Fe_{0.31}Zn_{0.69}F_2$ using magnetization and dynamic susceptibility measurements. However, the broad line shapes that indicate the glassy behavior were not observed in $Fe_{0.31}Zn_{0.69}F_2$ with neutron-scattering techniques.[21] It is of interest to note that neutron-scattering measurements[37] at the percolation threshhold in $Mn_{0.25}Zn_{0.75}F_2$ did not indicate any glassy behavior in contrast to $Fe_{0.25}Zn_{0.75}F_2$. This discrepancy may be due to an improper background subtraction[35] in the case of $Mn_{0.25}Zn_{0.75}F_2$, and this should be investigated further.

This work has been supported by DOE Grant No. DE-FG03-87ER45324 and by ORNL, which is managed by Lockheed Martin Energy Research Corp. for the U.S. DOE under Contract No. DE-AC05-96OR22464. One of us (F.C.M.) also acknowledges the support of CAPES, CNPq, FACEPE and FINEP (Brazilian agencies).

[1] For reviews, see D.P. Belanger and A.P. Young, J. Magn. Magn. Mater. **100**, 272 (1991); D.P. Belanger, in *Spin Glasses and Random Fields*, edited by A.P. Young (World Scientific, Singapore, 1998), p. 251; T. Nattermann, in *Spin Glasses and Random Fields*, edited by A.P. Young (World Scientific, Singapore, 1998), p. 277.

[2] J.W. Essam, Rep. Prog. Phys. **43**, 833 (1980).

[3] D. Stauffer and A. Aharony, *Introduction to Percolation, 2nd ed.* (Taylor & Francis, London, 1994).

[4] O. Nikotin, P.A. Lindgard, and O.W. Dietrich, J. Phys. C **2**, 1168 (1969).

[5] M.T. Hutchings, B.D. Rainford, and H.J. Guggenheim, J. Phys. C **3**, 307 (1970).

[6] F.C. Montenegro, A.R. King, V. Jaccarino, S.-J. Han, and D.P. Belanger, Phys. Rev. B **44**, 2155 (1991).

[7] C.A. Ramos, A.R. King, and V. Jaccarino, Phys. Rev. B **37**, 5483 (1988).

[8] S. Fishman and A. Aharony, J. Phys. **12**, L729 (1979).

[9] J.L. Cardy, Phys. Rev. B **29**, 505 (1984).

[10] H. Rieger, Phys. Rev. B **52**, 6659 (1995).

[11] F.C. Montenegro, K.A. Lima, M.S. Torikachvili, and A.H. Lacerda, J. Magn. Magn. Mater. **177-181**, 145 (1998).

[12] F.C. Montenegro, K.A. Lima, M.S. Torikachvili, and A.H. Lacerda, in *Magnetic Materials and their Applications*, Proceedings of the Fourth Latin American Workshop on Magnetism, edited by F.P. Missell [Mater. Sci. Forum **302-303**, 371 (1999).

[13] A. Rosales-Rivera, J.M. Ferreira, and F.C. Montenegro, Europhys. Lett. **50**, 264 (2000).

[14] R.J. Birgeneau, J. Magn. Magn. Mater. **177-181**, 1 (1998).

[15] R.J. Birgeneau, Q. Feng, Q.J. Harris, J.P. Hill, A.P. Ramirez, and T.R. Thurston, Phys. Rev. Lett. **75**, 1198 (1995).

[16] D.P. Belanger, W. Kleemann, and F.C. Montenegro, Phys. Rev. Lett. **77**, 2341 (1996).

[17] C. Ro, G. Grest, C. Sokoulis, and K. Levin, Phys. Rev. B **31**, 1682 (1985).

[18] J.R.L. de Almeida and R. Bruinsma, Phys. Rev. B **35**, 7267 (1987).

[19] U. Nowak and K.D. Usadel, Phys. Rev. B **44**, 7426 (1991); J. Magn. Magn. Mater. **104-107**, 179 (1992).

[20] F.C. Montenegro, U.A. Leitao, M.D. Coutinho-Filho, and S.M. Rezende, J. Appl. Phys. **67**, 5243 (1990).

[21] D.P. Belanger, W.E. Murray, F.C. Montenegro, A.R. King, V. Jaccarino, and R.W. Erwin, Phys. Rev. B **44**, 2161 (1991).

[22] Z. Slanic, D.P. Belanger, and J.A. Fernandez-Baca, J. Magn. Magn. Mater. **177-81**, 171 (1997).

[23] F.C. Montenegro, J.C.O. de Jesus, F.L.A. Machado, E. Montarroyos, and S.M. Rezende, J. Magn. Magn. Mater. **104**, 277 (1992).

[24] D.P. Belanger and H. Yoshizawa, Phys. Rev. B **47**, 5051 (1993).
[25] F.C. Montenegro, S.M. Rezende, and M.D. Coutinho-Filho, J. Appl. Phys. **63**, 3755 (1988).
[26] K. Jonason, C. Djurberg, P. Nordblad, and D.P. Belanger, Phys. Rev. B **56**, 5404 (1997).
[27] J. Satooka and A. Ito, J. Magn. Magn. Mater. **177-181**, 103 (1998).
[28] K. Jonason, P. Nordblad, and F.C. Montenegro (unpublished).
[29] B.W. Southern, A.P. Young, and P. Pfeuty, J. Phys. C **12**, 683 (1979).
[30] E.P. Raposo, M.D. Coutinho-Filho, and F.C. Montenegro, Europhys. Lett. **29**, 507 (1995); J. Magn. Magn. Mater. **154**, L155 (1996).
[31] C.L. Henley, Phys. Rev. Lett. **54**, 2030 (1985).
[32] A.N. Bazhan and S.V. Petrov, Zh. Éksp. Teor. Fiz. **80**, 669 (1981) [Sov. Phys. JETP **53**, 337 (1981)]; **86**, 2159 (1983) [**59**, 1269 (1984)].
[33] Schulhoff *et al.* (Ref. 34) showed that the measure of the static approximation is the neutron energy times the inverse correlation length. They established in pure MnF_2 that the static approximation was well satisfied for energies above 56 meV with κ as small as 0.002 rlu, yielding a parameter 0.1 meV rlu. For experiments with larger values of this parameter, the static approximation should hold. Our minimum value of κ is greater than 0.1 rlu, which together with the energy 14.7 meV yields a minimum parameter value greater than 0.15 meV rlu, well within the static approximation, assuming that the same range works as well in $Mn_xZn_{1-x}F_2$ as in MnF_2. We note that Schulhoff *et al.* did not determine the minimum value of the parameter satisfying the static approximation, and it may be significantly less than the minimum value they investigated.
[34] M.P. Schulhoff, P. Heller, R. Nathans, and A. Linz, Phys. Rev. B **1**, 2304 (1970).
[35] Schulhoff *et al.* (Ref. 34) studied pure MnF_2 and were able to separate the noncritical transverse-fluctuation scattering background from the critical scattering due to longitudinal fluctuations. They did this by measuring the scattering at (001), which involves only transverse magnetic scattering since the anisotropy is along the *c* axis direction, and subtracting it from the (100) scattering, which involves both transverse and longitudinal scattering. Extinction effects and sample shape effects prevent a direct subtraction. The amplitude of the transverse scattering was therefore treated as a fitting variable to allow the subtraction. This allowed a more accurate treatment of the critical line shape at very small κ. This procedure cannot be applied to the present case of $Mn_{0.35}Zn_{0.65}F_2$ for several reasons. The source of the anisotropy is the dipolar fields of neighboring spins. Since the local environment of the spins in the dilute case causes the local anisotropy to deviate significantly from the *c* axis, scattering from longitudinal fluctuations is not restricted to (100) as in the pure case. Hence, there is no clear procedure for making this correction in the dilute case. What is clear is that the use of the corrections of Schulhof *et al.* in highly diluted systems would be incorrect and would certainly lead to unreliable results. This is probably the case for the results reported (Ref. 37) for $Mn_{0.25}Zn_{0.75}F_2$ from an analysis that used the approach of Schulhof *et al.*, as noted in the conclusion of this manuscript. In addition to the problems in separating the transverse fluctuations from the longitudinal ones due to the nonuniaxial local anisotropies, a large noncritical component of the scattering at (100) in $Mn_{0.35}Zn_{0.65}F_2$ comes from spins that do not contribute to the phase transition. This is evident from specific-heat (Ref. 7) measurements and from the small amplitude of the scattering line shapes. The noncritical component also prevents a detailed critical behavior analysis of the line shapes. Hence, we only compare line-shape analyses with random-exchange behavior to suggest consistency, without making strong arguments about the precise critical values obtained. To go further would require much deeper understanding of the nature of the ordering in the highly dilute sample in the presence of random anisotropy and exchange frustration.
[36] F.C. Montenegro, A. Rosales-Rivera, J.C.O. de Jesus, E. Montarroyos, and F.L.A. Machado, Phys. Rev. B **51**, 5849 (1995).
[37] R.A. Cowley, G. Shirane, R.J. Birgeneau, E.C. Svensson, and H.J. Guggenheim, Phys. Rev. B **22**, 4412 (1980).
[38] D.P. Belanger and H. Yoshizawa, Phys. Rev. B **35**, 4823 (1987).
[39] D.P. Belanger, A.R. King, and V. Jaccarino, Phys. Rev. B **34**, 452 (1986).
[40] H.G. Ballesteros, L.A. Fernández, V. Martín-Mayor, A. Munoz Sudupe, G. Parisi, and J.J. Ruiz-Lorenzo, Phys. Rev. B **58**, 2740 (1998).
[41] D.P. Belanger, A.R. King, I.B. Ferreira, and V. Jaccarino, Phys. Rev. B **37**, 226 (1987).
[42] N. Rosov, A. Kleinhammes, P. Lidbjork, C. Hohenemser, and M. Eibschutz, Phys. Rev. B **37**, 3265 (1988).